THE JOURNAL OF BIOLOGICAL CHEMISTRY VOL. 286, NO. 2, pp. 1283–1291, January 14, 2011

p38 MAPK Activation Is Downstream of the Loss of Intercellular Adhesion in Pemphigus Vulgaris*[S]

Received for publication, August 6, 2010, and in revised form, October 17, 2010 Published, JBC Papers in Press, November 15, 2010, DOI 10.1074/jbc.M110.172874

Xuming Mao[‡], Yasuyo Sano[§], Jin Mo Park[§], and Aimee S. Payne[‡1]

From the [‡]Department of Dermatology, University of Pennsylvania, Philadelphia, Pennsylvania 19104 and the [§]Cutaneous Biology Research Center, Massachusetts General Hospital and Harvard Medical School, Charlestown, Massachusetts 02129

Pemphigus vulgaris (PV) is a potentially fatal blistering disease characterized by autoantibodies against the desmosomal adhesion protein desmoglein (Dsg) 3. Whether autoantibody steric hindrance or signaling through pathways such as p38 MAPK is primary in disease pathogenesis is controversial. PV mAbs that cause endocytosis of Dsg3 but do not dissociate keratinocytes because of compensatory adhesion by Dsg1 do not activate p38. The same mAbs plus exfoliative toxin to inactivate Dsg1 but not exfoliative toxin alone activate p38, suggesting that p38 activation is secondary to loss of adhesion. Mice with epidermal p38α deficiency blister after passive transfer of PV mAbs; however, acantholytic cells retain cell surface Dsg3 compared with wild-type mice. In cultured keratinocytes, p38 knockdown prevents loss of desmosomal Dsg3 by PV mAbs, and exogenous p38 activation causes internalization of Dsg3, desmocollin 3, and desmoplakin. p38α MAPK is therefore not required for the loss of intercellular adhesion in PV, but may function downstream to augment blistering via Dsg3 endocytosis. Treatments aimed at increasing keratinocyte adhesion could be used in conjunction with immunosuppressive agents, potentially leading to safer and more effective combination therapy regimens.

Pemphigus vulgaris (PV)[2] is a potentially fatal autoimmune blistering disorder caused by autoantibodies to keratinocyte cell adhesion proteins known as desmogleins (1). The pathognomonic histologic finding in PV is suprabasal acantholysis, or the detachment of intact keratinocytes from each other because of loss of intercellular adhesion. A characteristic clinical finding in PV is Nikolsky's sign, in which blisters can be induced in otherwise normal-appearing skin by applying pressure or mechanical shear force, reflecting the loss of intercellular adhesion even in skin without overt blisters (2).

PV autoantibodies primarily target desmoglein (Dsg) 3, a transmembrane adhesion molecule of desmosomes (3). Passive transfer experiments using neonatal mice have established the pathogenicity of the anti-Dsg3 autoantibodies in PV (4, 5). The anatomic site of blister formation is thought to be due to the tissue-specific expression patterns of different Dsg isoforms, also known as the desmoglein compensation theory. Dsg3 is expressed by basal keratinocytes of mucosa and skin, whereas Dsg1 is expressed by basal keratinocytes in skin but not mucosa (6, 7). Therefore, patients with Dsg3 autoantibodies demonstrate blistering in the mucosa, where compensatory adhesion by Dsg1 is not present (mucosal-dominant PV). In some patients who progress to develop Dsg1 in addition to Dsg3 autoantibodies, suprabasal blisters appear in both the mucosa and skin (mucocutaneous PV) (8–10).

Epitope mapping studies have shown that pathogenic PV autoantibodies preferentially bind the amino-terminal domain of Dsg3 that is predicted to form the transadhesive interface between cells, based on analogy to ultrastructural models for the classical cadherins (11–13). PV IgG has also been shown to directly inhibit Dsg3 homophilic interactions *in vitro* (14). These data have supported the "steric hindrance" model of disease, in which direct interference with Dsg3 interactions causes the loss of intercellular adhesion.

The loss of intercellular adhesion in PV has been mechanistically linked to the endocytosis and degradation of Dsg3 (15–18), although it has been debated whether endocytosis is the result or the cause of the loss of intercellular adhesion. Additionally, other studies have shown that inhibition of various signaling pathways can prevent blister formation in the passive transfer mouse model, questioning the primacy of steric hindrance in disease pathogenesis (19). p38 MAPK is phosphorylated in human keratinocytes treated with PV IgG and in PV skin lesions (20, 21). Inhibitor studies using SB202190 and related compounds have suggested that p38 activation is necessary for blister formation in the passive transfer mouse model (22) as well as for PV IgG-mediated Dsg3 internalization (23).

p38 is a member of the MAPK family, best characterized for its role in regulating the cellular response to a variety of infectious and environmental stimuli, including thermal, osmotic, and oxidative stress (24–27). Four p38 isoforms (α, β, γ, and δ) have been identified (28–31). The α, β, and δ isoforms have been detected at the RNA level in cultured human keratinocytes (32), whereas mouse epidermal keratinocytes express the α, γ, and δ isoforms (33). The four isoforms share structural and biochemical properties, including a dual Thr/Tyr motif activated by phosphorylation. Only the α and β isoforms are susceptible to inhibition by pyridinyl imidazoles

* This work was supported, in whole or in part, by National Institutes of Health Grants AR053505 and AR057001 from NIAMS (to A. S. P.) and Grant AI074957 from NIAID (to J. M. P.). This work was also supported by Penn Skin Disease Research Core Grant AR057217.

[S] The on-line version of this article (available at http://www.jbc.org) contains supplemental Figs. S1–S4 and Tables S1 and S2.

[1] To whom correspondence should be addressed: 217A Clinical Research Bldg., 415 Curie Blvd., Philadelphia, PA 19104. Fax: 215-573-7173; E-mail: paynea@mail.med.upenn.edu.

[2] The abbreviations used are: PV, pemphigus vulgaris; Dsg, desmoglein; PHEK, primary human epidermal keratinocyte(s); eGFP, enhanced GFP; KO, knock-out; ETA, exfoliative toxin A.

such as SB202190 (34, 35); however, these ATP-binding site inhibitors have also been shown to affect protein kinases other than p38 (36). To further define the role of p38 in desmosomal cell adhesion and PV, we studied the effects of pathogenic PV mAbs in normal and p38-silenced primary human keratinocytes as well as mice with a K14-Cre-mediated deletion of p38α MAPK in the epidermis.

EXPERIMENTAL PROCEDURES

Antibodies and Reagents—Primary antibodies included mouse monoclonal anti-p38 and anti-phospho-p38 (Thr-180/Tyr-182) and rabbit anti-p38α (Cell Signaling Technology), mouse monoclonal anti-Dsg3 (5G11, Invitrogen), rabbit polyclonal anti-Dsg3 (H-145, Abcam), mouse anti-desmoplakin (BioDesign International), mouse monoclonal anti-Dsc3 (U114, Meridian Life Science Inc.), rabbit polyclonal anti-Dsc3 (H-50, Santa Cruz Biotechnology Inc.), mouse monoclonal anti-keratin (Zymed Laboratories Inc.), mouse monoclonal anti-plakoglobin (11E4, anti-γ-catenin, Chemicon), and mouse anti-EEA-1 (BD Biosciences).

Secondary antibodies or reagents included HRP-conjugated donkey anti-mouse or anti-rabbit IgG (Jackson ImmunoResearch Laboratories), Alexa 488-conjugated donkey anti-rabbit IgG, Alexa 488-conjugated goat anti-mouse and rabbit IgG, and Alexa 594-conjugated goat anti-mouse, rat, and rabbit IgG (Molecular Probes).

PV mAbs were produced as described previously (37). The p38 inhibitor (SB202190) and its structural analog (SB202474) were a generous gift from Dr. John Seykora.

Cell Culture and Treatments—Primary human epidermal keratinocytes (PHEK) isolated from neonatal foreskin were obtained from the Penn Skin Disease Research Center. Cells from passages 4–5 were propagated in defined keratinocyte serum-free medium (Invitrogen) containing 0.07 mM $CaCl_2$ and penicillin/streptomycin (Invitrogen) and maintained in a humidified incubator with 5% CO_2 at 37 °C. Cells were incubated with 0.4 mM calcium for 16 h to promote desmosome assembly, followed by treatment with PV mAbs, anisomycin, or H_2O_2. For p38 inhibition assays, cells were treated with 2 μM SB202190 or its inactive analog SB202474, followed by 0–200 μg/ml PV mAbs, 0–200 μM H_2O_2, or 0–100 μg/ml anisomycin.

Immunofluorescence Studies—PHEK were seeded on coverslips preincubated with rat tail collagen (Sigma). Cells were treated with PV mAbs in defined keratinocyte serum-free medium containing 1.2 mM calcium for the indicated amount of time and then fixed in PBS containing 4% paraformaldehyde (freshly diluted from a 20% paraformaldehyde solution, Electron Microscopy Sciences) for 20 min at 4 °C, or with ice-cold methanol or methanol/acetone (1:1) for 15 min at 4 °C. For cells fixed with 4% paraformaldehyde, a 3-min incubation with PBS containing 0.2% Triton X-100 was used for cell permeabilization. Cells were blocked in PBS containing 2% BSA for 60 min at room temperature or overnight at 4 °C, followed by incubation with primary antibodies in blocking solution for 1 h at room temperature. After three washes in PBS, cells were incubated with secondary antibodies diluted 1:200 in blocking solution for 30–60 min at room temperature. Nuclear staining was performed with DAPI (Sigma) or with ProLong Gold antifade reagent with DAPI (Molecular Probes). Immunofluorescence was visualized with an Olympus BX61 microscope. Images were acquired using Slidebook 4.2 software (Olympus) and a Hamamatsu Orca ER camera, using consistent time exposures among samples. Nearest neighbor deconvolution was performed on the acquired images.

For cell surface labeling of Dsg3, PHEK were first cultured for 18 h in defined keratinocyte serum-free medium containing 0.4 mM calcium to promote desmosome assembly. Cells were incubated in the same medium containing a nonpathogenic anti-Dsg3 mAb conjugated with enhanced GFP (eGFP; provided by John R. Stanley) at 4 °C for 1 h, washed with PBS, and subsequently incubated with 200 μM H_2O_2 or 200 μg/ml anisomycin at 37 °C for 0–16 h. Cells were fixed with 4% paraformaldehyde without permeabilization and visualized using an Olympus BX61 microscope.

For mouse skin tissue, binding of PV mAbs after passive transfer was confirmed in mouse skin by direct immunofluorescence using anti-human IgG conjugated with FITC (Invitrogen). Costaining of Dsg3 was performed using a mouse monoclonal anti-Dsg3 antibody (5G11), followed by Alexa Fluor 594-conjugated anti-mouse IgG. Immunofluorescence was visualized using a Leica TCS SP2 confocal microscopy system (20× objective lens, 0.7 numerical aperture) using excitation wavelengths of 488 and 561 nm and detection wavelengths of 500–540 and 575–675 nm, respectively. The relative amount of cell surface Dsg3 was evaluated using ImageJ analysis of confocal images. 100 keratinocytes from skin sections of three WT and four knock-out (KO) mice were measured by region of interest. The relative amount of cell surface Dsg3 was calculated as (total cellular signal intensity − intracellular signal intensity)/total cellular signal intensity, normalizing the mean value for KO mice to 1.0.

Cell Fractionation and Immunoblotting—PHEK were cultured to 90–100% confluence in defined keratinocyte serum-free medium with 5% CO_2 at 37 °C before experiments. After treatments, cells were chilled on ice and washed with ice-cold PBS containing calcium and magnesium (Dulbecco's PBS, Mediatech, Inc.). For cell fractionation assays, cells were lysed in buffer containing 1% Triton X-100, 10 mM Tris-HCl (pH 7.5), 140 mM NaCl, 5 mM EDTA, and 2 mM EGTA with protease inhibitors (P8340, Sigma) for 15 min on ice, followed by centrifugation at 16,000 × *g* for 20 min at 4 °C. The resulting Triton X-100-soluble supernatant was collected as the cytosol/membrane (nondesmosomal) fraction. The Triton X-100-insoluble pellets (containing desmosomal fractions) were solubilized in Laemmli sample buffer containing 5% β-mercaptoethanol. Total protein was determined by protein assay (RC-DC, Bio-Rad), and 50 μg of each sample fraction was separated by SDS-PAGE. Proteins were transferred to nitrocellulose, and membranes were incubated with primary antibodies diluted in PBS and 5% milk. Blots were washed with PBS containing 0.1% Tween 20 and then incubated with either HRP-conjugated goat anti-mouse (Bio-Rad) or donkey anti-mouse (Jackson ImmunoResearch Laboratories) secondary antibodies diluted in PBS and 5% milk. Blots were developed using ECL Plus reagent (Amersham Biosciences).

Quantitation of the relative increase in p38 activity by immunoblotting (as a -fold increase over basal p38 phosphorylation) was performed using Scion Image 4.0.3.2 and normalized for protein expression in each assay. Statistical analysis was conducted using one-way analysis of variance.

RNA Interference—Transfections of p38 pool or control siRNAs (Cell Signaling Technology) into primary human epidermal keratinocytes were performed using Lipofectamine 2000 transfection reagent (Invitrogen) according to the manufacturer's protocols. Cells transfected with siRNA were treated with PV mAbs or H_2O_2 for 4 h in the presence of 1.2 mM calcium 48 h after transfection and subsequently harvested for analysis.

Neonatal Mouse Passive Transfer—p38 fl/fl;+/+ (WT) or p38 fl/fl;K14cre/+ (KO) mice on a C57Bl/6J background were used for passive transfer studies (33). Newborn mice (1–2 days old) weighing between 1.2 and 1.8 g were injected subcutaneously between the shoulder blades using a 1-ml insulin syringe. Each animal received 10–40 μg of purified NP2 or P1 IgG and was sacrificed 6 h later for evaluation. Skin sections were fixed in 10% phosphate-buffered formalin (Fisher) for histology. Skin was also harvested for direct immunofluorescence by embedding and freezing in O.C.T. compound (Electron Microscopy Sciences). Blood was collected, and the serum was tested using Dsg3 ELISA (MBL International) to determine the index value of circulating PV IgG for each injection. Tails were collected for DNA extraction and genotyping as described previously (33).

Histology and Immunohistochemistry—Formalin-fixed, paraffin-embedded mouse skin sections, 4–6 μm thick, were stained with hematoxylin and eosin according to standard procedures for histologic evaluation of blister formation after passive transfer of PV IgG. For UV radiation experiments, WT mice were exposed to a one-time UVB dose of 500 mJ/cm^2, and skin was harvested 24 h after exposure. Immunohistochemical staining was performed to evaluate p38 activation in mouse epidermis. Briefly, paraffin-embedded sections were heated at 80 °C for 30 min, followed by deparaffinization and antigen retrieval in citrate buffer (pH 7) at 100 °C for 7 min. The sections were treated with 0.3% H_2O_2 (Sigma) for 1 h at room temperature and blocked with 2% BSA (Sigma) for 1 h at room temperature. Rabbit anti-phospho-p38 or rabbit anti-p38α primary antibodies were incubated with skin sections overnight at 4 °C, followed by peroxidase-conjugated donkey anti-rabbit IgG for 1 h at room temperature. Sections were developed using a liquid diaminobenzidine substrate kit (Invitrogen).

RESULTS

Pathogenic PV mAbs That Cause Internalization of Dsg3 and the Loss of Intercellular Adhesion but Not Those That Cause Internalization of Dsg3 without the Loss of Intercellular Adhesion Activate p38 MAPK—PV serum IgG is heterogeneous, containing pathogenic, nonpathogenic, and many unrelated antibodies. Previously, we isolated pathogenic and nonpathogenic anti-Dsg3 mAbs from PV patients (37). Pathogenicity is defined by the ability of mAbs to cause suprabasal acantholytic blistering in human skin explants and/or passive transfer to neonatal mice, in addition to dissociation of cultured human keratinocytes. Prior studies have shown that pathogenic but not nonpathogenic PV mAbs also cause endocytosis of Dsg3, but not the related desmosomal adhesion protein desmocollin 3, thereby disrupting desmosome assembly (17).

In cultured primary human keratinocytes, as in the epidermis, both Dsg3 and Dsg1 must be inactivated to cause cell dissociation. Therefore, pathogenic mAbs that recognize both Dsg3 and Dsg1 cause cell dissociation of cultured keratinocytes, suprabasal blisters in human skin, and Dsg3 endocytosis, whereas pathogenic mAbs that recognize only Dsg3 will cause Dsg3 endocytosis but will not cause cultured cell dissociation or blisters in human skin unless compensatory adhesion by Dsg1 is also inactivated, by either pathogenic anti-Dsg1 autoantibodies or staphylococcal exfoliative toxin, which cleaves Dsg1 (38–40). Supplemental Table S1 summarizes the antigen specificity of the mAbs used in our study, including AK23, a pathogenic anti-Dsg3 mAb isolated from an active immune mouse model of PV (41).

We evaluated four pathogenic and two nonpathogenic anti-Dsg3 mAbs for their ability to activate p38 in PHEK as determined by immunoblotting of keratinocyte lysates with antibodies specific for Thr/Tyr-phosphorylated p38 (all four isoforms) using total p38 as a loading control. Pathogenic antibodies P1 and P3, which cause Dsg3 internalization and the loss of intercellular adhesion, activated p38 (Fig. 1*A*). P1 mAb activated p38 in a dose-dependent manner, which was comparable among monovalent single-chain variable fragment, IgG1, and IgG4 forms of P1 mAb (supplemental Fig. S1), indicating that cross-linking of Dsg molecules is not required for p38 activation.

In contrast, nonpathogenic antibodies NP1 and NP2, as well as pathogenic antibodies AK23 and P2, which cause Dsg3 internalization but not keratinocyte dissociation because of compensatory adhesion by Dsg1, did not activate p38 (Fig. 1*A*). The same mAbs plus low-dose exfoliative toxin A (ETA) to inactivate Dsg1 and cause the loss of keratinocyte adhesion, but not low-dose ETA alone, activated p38 (Fig. 1, *B* and *C*). These findings indicate that p38 activation is not required for PV mAb-induced Dsg3 endocytosis and also suggest that p38 activation is secondary to the loss of intercellular adhesion.

Mice with a Targeted Deletion of p38α MAPK in the Epidermis Demonstrate Loss of Intercellular Adhesion after Passive Transfer of PV mAbs—We next evaluated whether mice with a K14-Cre-mediated deletion of p38α in the epidermis (KO, p38 fl/fl;K14cre/+) were susceptible to experimental PV using wild-type littermates (WT, p38 fl/fl;+/+) as controls. The efficiency of p38α deletion in skin keratinocytes is essentially complete, as determined by immunoblotting of epidermal keratinocyte lysates and p38α-specific immunohistochemistry of blistered skin from WT and KO mice (supplemental Fig. S2). Three WT and two KO mice injected with 40 μg of nonpathogenic NP2 IgG demonstrated no evidence of gross or histologic blistering (Fig. 2, *A* and *B*). Five WT and three KO mice injected with 40 μg of pathogenic P1 IgG all demonstrated Nikolsky-positive blisters and suprabasal acantholysis on histology (Fig. 2, *A* and *B*). To evaluate whether KO mice

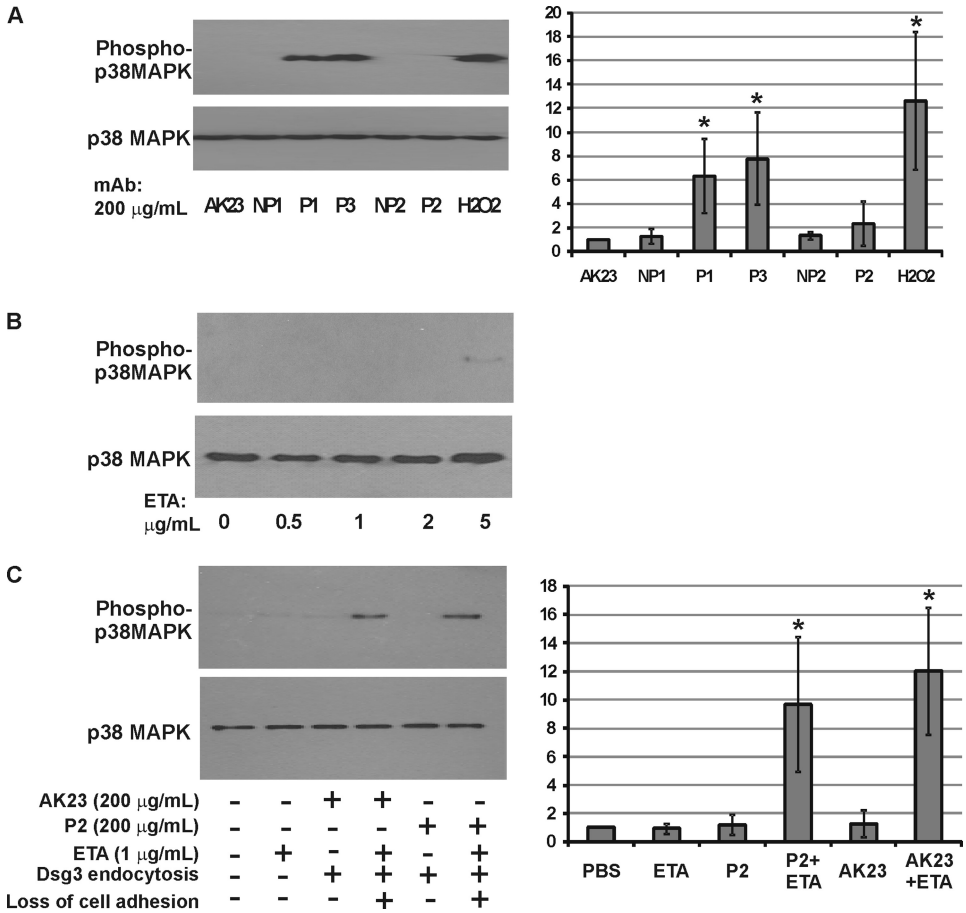

FIGURE 1. **PV mAbs that cause the loss of intercellular adhesion, but not those that cause internalization of Dsg3 without loss of intercellular adhesion, activate p38 MAPK.** *A*, survey of pathogenic and nonpathogenic PV mAbs on activation of p38. PHEK were treated with 200 μg/ml mAbs or 100 μM H_2O_2 for 2 h, followed by lysis of cells with Laemmli sample buffer containing 5% β-mercaptoethanol. p38 phosphorylation (*upper panel*) and total p38 protein (*lower panel*) levels were determined by immunoblotting using antibodies specific to phospho-Thr-180/Tyr-182 p38 and p38, respectively. P1 and P3 pathogenic mAbs cause Dsg3 internalization and loss of intercellular adhesion, whereas P2 and AK23 pathogenic mAbs cause Dsg3 internalization only (loss of intercellular adhesion in cultured keratinocytes depends on simultaneous inactivation of Dsg1). NP1 and NP2 are nonpathogenic PV mAbs. *B*, ETA, which cleaves Dsg1, weakly activates p38 at high doses. PHEK were treated with increasing doses of ETA for 2 h and assayed for p38 activation as described above. *C*, synergistic effect of ETA and P2 or AK23 mAbs on p38 activation. Cells were treated with PV mAbs (200 μg/ml), 1 μg/ml ETA alone, or PV mAb plus 1 μg/ml ETA. p38 activation was observed only under experimental conditions causing the loss of intercellular adhesion. For *A* and *C*, the -fold increase in p38 phosphorylation from three independent experiments was quantitated (normalizing basal phosphorylation to 1.0). *Error bars* indicate 1 S.D. above and below the mean value. *, $p < 0.05$ (by analysis of variance).

may demonstrate a lower threshold for blister induction compared with WT mice, we passively transferred decreasing doses of pathogenic P1 IgG to neonatal mice. After passive transfer of 20 μg, four/five WT mice and three/three KO mice demonstrated gross blisters with histology demonstrating suprabasal acantholysis. After passive transfer of 10 μg, zero/three WT and three/four KO mice demonstrated gross blisters, although three/three WT and four/four KO mice demonstrated suprabasal acantholysis on histology (summarized in supplemental Table S2). These findings indicate that p38α MAPK is not required for the loss of intercellular adhesion in the passive transfer neonatal mouse model of PV.

p38 MAPK Activation Is Observed in Lesional but Not Nonlesional Keratinocytes from Wild-Type and, to a Lesser Extent, p38α-deficient Mouse Epidermis—To determine whether activated p38 is detectable in epidermal keratinocytes of WT and KO mice, we performed immunohistochemical staining for Thr/Tyr-phosphorylated p38. As a positive control for staining, UVB irradiation resulted in a marked increase in phospho-p38 staining in mouse skin compared with nonirradiated mice (Fig. 2*C*). Significant p38 activation was observed in keratinocytes in the blister roof and base of WT mice (indicated by *arrows*) injected with 40 μg of P1 mAb compared with keratinocytes in perilesional epidermis. No p38 activation was detected in perilesional keratinocytes in p38α-deficient epidermis. Focal phospho-p38 staining (due to remaining p38γ and/or p38δ) was observed in lesional keratinocytes in p38α-deficient epidermis (indicated by *arrows*).

Dsg3 Localization Differs in Acantholytic Cells of p38α-deficient and Wild-type Mouse Epidermis—To evaluate the *in vivo* effects of p38α deficiency on PV mAb-induced internalization of cell surface Dsg3, we performed confocal immunofluorescence microscopy on the skin of mice injected with pathogenic P1 IgG. P1 IgG and mouse Dsg3 were stained in skin sections from three KO and five WT mice injected with 40 μg of P1 IgG. In acantholytic keratinocytes of WT mice, Dsg3 as well as IgG cell surface staining was disrupted (Fig. 2*D*). In KO mice, acantholytic keratinocytes retained Dsg3

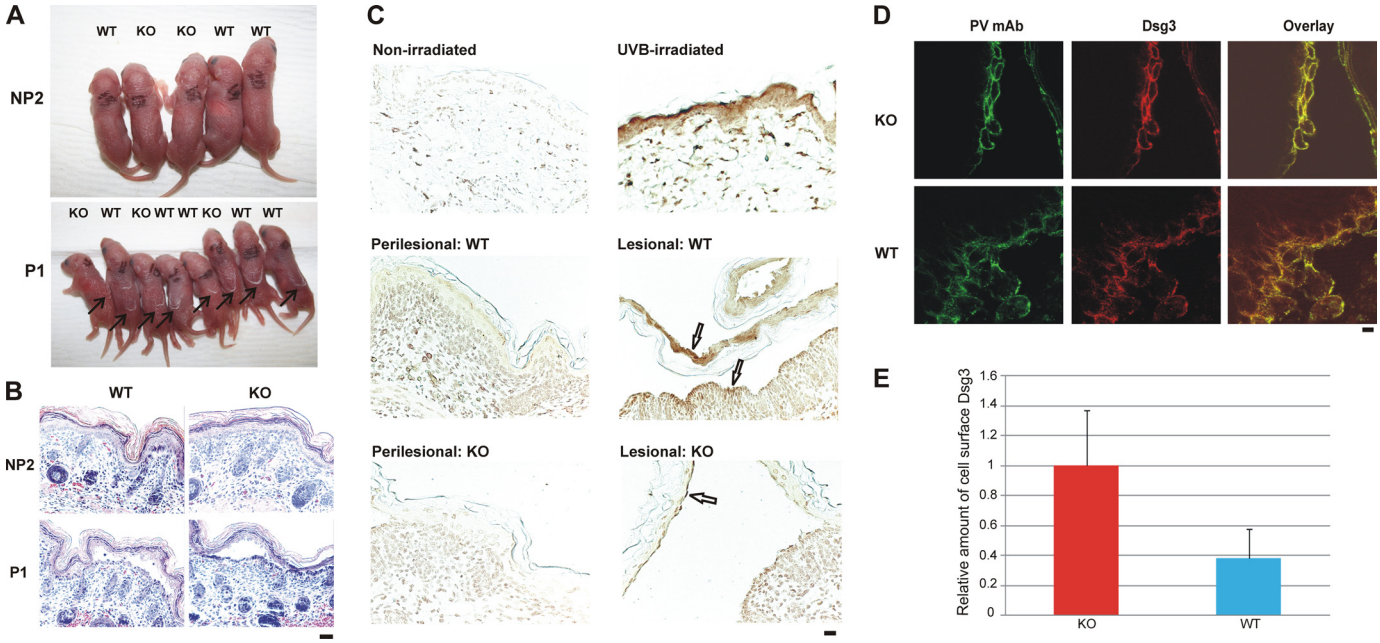

FIGURE 2. **Mice with a targeted deletion of p38α MAPK in the epidermis are susceptible to experimental PV.** *A*, gross blister formation after passive transfer of pathogenic PV mAbs. p38 fl/fl;K14cre/+ (KO) and p38 fl/fl;+/+ (WT) mice were injected subcutaneously with 40 μg of nonpathogenic (NP2) or pathogenic (P1) PV IgG. Both WT and KO mice developed gross blisters (indicated by *arrows*) after P1 IgG passive transfer. *B*, P1 mAb causes suprabasal PV blisters in both WT and KO mice. Mice injected with nonpathogenic (NP2) PV mAb did not develop blisters. 12 of 13 WT mice and eight of eight KO mice injected with P1 mAb developed histologic blisters with suprabasal acantholysis typical of PV. *Scale bar* = 100 μm. *C*, p38 is activated in lesional but not perilesional keratinocytes of mouse epidermis after P1 mAb passive transfer. UVB irradiation led to phosphorylation of p38 in mouse epidermis. Activated p38 was markedly increased in lesional compared with perilesional keratinocytes from WT mice. Focal p38 activation was detected in lesional keratinocytes from p38α-deficient epidermis. *Scale bar* = 100 μm. *D*, confocal immunofluorescence microscopy of WT and KO mouse skin after pathogenic P1 mAb passive transfer. Localization of Dsg3 (*green*) and P1 IgG (*red*) is shown. *Scale bar* = 10 μm. *E*, quantification of cell surface Dsg3. The relative amount of cell surface Dsg3 was significantly increased in p38α-deficient skin keratinocytes compared with those in WT mice ($p < 0.01$ (Student's *t* test)). Confocal immunofluorescence experiments were performed three times; *error bars* indicate 1 S.D. the mean.

and P1 IgG cell surface localization, suggesting defects in PV mAb-induced internalization of Dsg3 in p38α-deficient keratinocytes. The cell surface localization of Dsg3 was significantly different between keratinocytes in WT and KO mice ($p < 0.01$ (Student's *t* test)) (Fig. 2*E*).

Activation of p38 Stimulates Dsg3 Endocytosis and Inhibition of p38 Activation Prevents PV mAb-induced Dsg3 Endocytosis—To further explore the relationship between p38 activation and Dsg3 endocytosis, we exogenously activated p38 in PHEK and determined the subcellular localization of Dsg3. In initial experiments, we determined the dose response of p38 activation to anisomycin and H_2O_2 (supplemental Fig. S4*A*). Treatment of primary human keratinocytes with anisomycin caused loss of cell surface Dsg3 and the desmosomal marker desmoplakin (Fig. 3*A*). Similar findings were observed after oxidative stress of PHEK with H_2O_2. Loss of cell surface desmocollin 3, the other major desmosomal cadherin expressed by basal keratinocytes, but not the adherens junction protein E-cadherin, was observed after anisomycin or H_2O_2 treatment of PHEK (Fig. 3*B*). To confirm that anisomycin or H_2O_2 stimulated internalization of cell surface Dsg3, we labeled cell surface Dsg3 using an eGFP-conjugated nonpathogenic anti-Dsg3 antibody that has been demonstrated previously not to cause endocytosis of Dsg3 (17). After incubation with the eGFP-conjugated antibody at 4 °C for 1 h, PHEK were washed and treated with anisomycin or H_2O_2. At 4 h and more significantly at 16 h, eGFP-labeled Dsg3 was internalized from the cell surface (Fig. 3*C*). No significant colocalization of Dsg3 and the early endosomal marker EEA-1 was observed after activation of p38 in PHEK by oxidative stress (supplemental Fig. S3).

To determine whether the effects of anisomycin, H_2O_2, and PV mAbs are dependent on p38 activation, we examined the effects of p38 inhibition and gene silencing in PHEK. Preliminary experiments confirmed that SB202190 but not its inactive analog SB202474 inhibited the activation of p38 MAPK by oxidative stress (supplemental Fig. S4*B*). Inhibition of p38 activation decreased the H_2O_2- or PV mAb-induced internalization of Dsg3 (Fig. 4*A*). To confirm that these effects were specific for p38, we used a siRNA approach to silence p38 MAPK gene expression. Transfection of PHEK with p38 and control siRNAs (the latter encoding green fluorescent protein) indicated a 70–90% transfection efficiency. Transfection of PHEK with p38 siRNA targeting all four isoforms abolished total p38 protein levels compared with PHEK transfected with control siRNA (Fig. 4*B*, *lowest panel*). Treatment of control siRNA-transfected PHEK with H_2O_2 or pathogenic P1 mAb depleted Dsg3, desmoplakin, and, to a lesser extent, plakoglobin in the Triton X-100-insoluble (desmosomal) fraction (Fig. 4*B*, *upper panels*). Treatment of control siRNA-transfected PHEK with H_2O_2 or pathogenic P1 mAb also resulted in the loss of Dsg3 but not the unrelated protein tubulin in the Triton X-100-soluble (nondesmosomal) fraction (Fig. 4*B*, *lower panels*). E-cadherin protein levels were slightly reduced in H_2O_2-treated but not P1 mAb-treated PHEK. Knockdown of p38 gene expression rescued the P1 mAb-induced and, to a

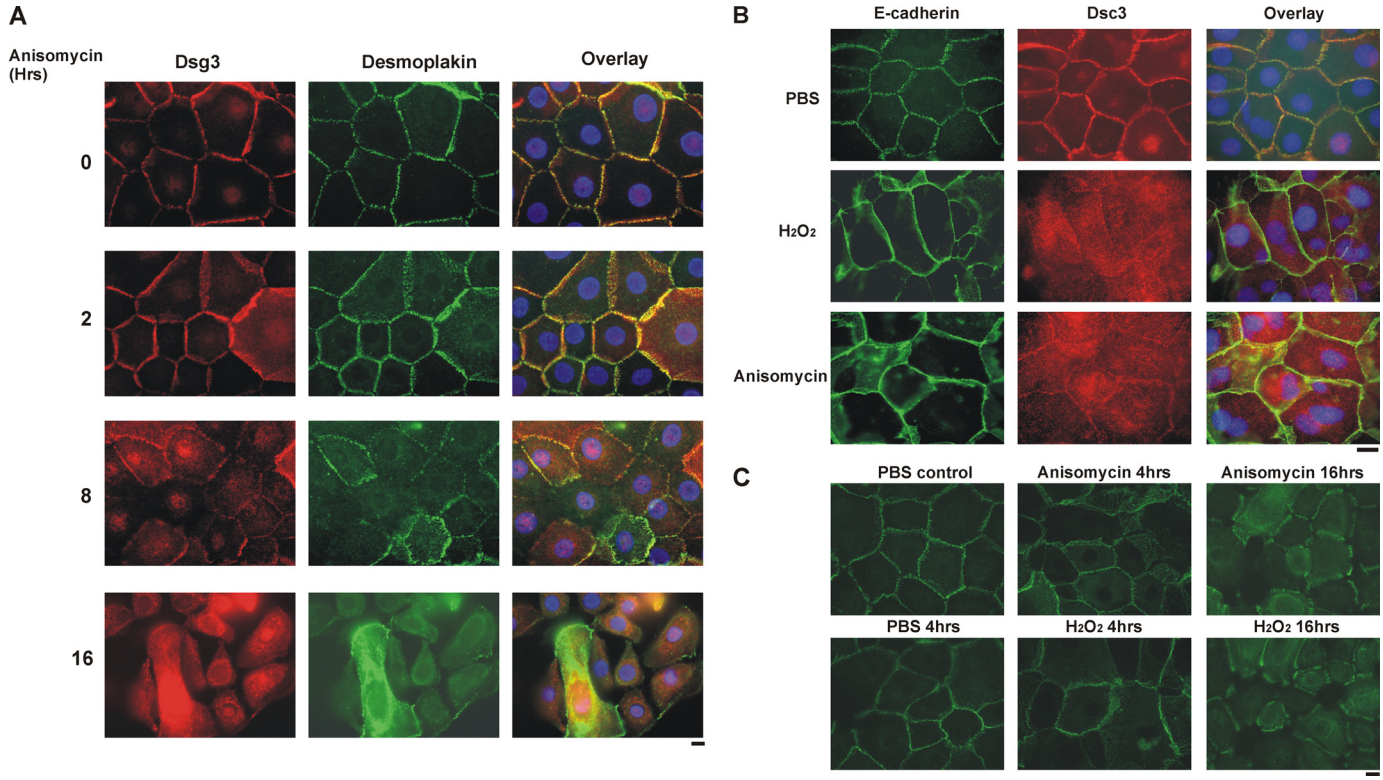

FIGURE 3. **Activation of p38 MAPK causes loss of desmosomal Dsg3.** *A*, anisomycin disrupts the desmosomal cell surface localization of Dsg3. PHEK were treated with 0.4 mM calcium for 16 h to induce desmosome assembly, followed by treatment with the p38 activator anisomycin (100 μg/ml) for the specified amount of time. The localization of Dsg3 (*red*) or the desmosomal marker desmoplakin (*green*) was visualized by immunofluorescence microscopy. Nuclei (*blue*) were stained with DAPI, as shown in image overlay. *Scale bar* = 10 μm. *B*, desmosomal proteins are preferentially disrupted by p38 activation. PHEK were treated with 200 μM H_2O_2 or 200 μg/ml anisomycin for 4 h in medium containing 1.2 mM calcium. Localization of the adherens junction protein E-cadherin and the desmosomal cadherin desmocollin 3 was evaluated by immunofluorescence microscopy. *Scale bar* = 10 μm. *C*, activation of p38 causes internalization of cell surface Dsg3. PHEK were cultured in medium containing 0.4 mM calcium for 18 h to promote desmosome assembly. Cells were then incubated in the same medium containing a nonpathogenic anti-Dsg3 mAb tagged with GFP at 4 °C for 1 h to label cell surface Dsg3. After washing with PBS, cells were treated with 200 μM H_2O_2 or 100 μg/ml anisomycin for 0–16 h. Cells were fixed without permeabilization, and the localization of surface-labeled Dsg3 was evaluated by immunofluorescence microscopy. *Scale bar* = 10 μm.

lesser extent, the H_2O_2-induced loss of Dsg3 in the Triton X-100-soluble and Triton X-100-insoluble fractions.

DISCUSSION

The relationship between p38 activation, Dsg3 endocytosis, and the loss of intercellular adhesion in PV has been difficult to determine. A major problem in comparing data from different laboratories is that PV IgG isolated from patients' sera is heterogeneous, containing a mixture of pathogenic and nonpathogenic mAbs that can recognize Dsg3 as well as other desmosomal cadherins, with serum titers varying between different patients and even within the same patient over time. We have previously shown that recombinant nonpathogenic anti-Dsg3 mAbs cloned from a PV patient bind Dsg3 but do not cause its endocytosis or interfere with its incorporation into the desmosome; in contrast, recombinant pathogenic PV mAbs cause endocytosis of newly synthesized Dsg3, impairing desmosome assembly and consequently desmosomal adhesion (17). The advantage of our approach is that we use well characterized pathogenic PV mAbs with nonpathogenic PV mAbs as controls, thereby avoiding potential heterogeneous effects caused by polyclonal patient IgG. Additionally, all prior studies on the role of p38 MAPK in PV have been performed using only pyridinyl imidazole inhibitors, which can inhibit kinases other than p38 (36). In the current study, we have more specifically investigated the role of p38 MAPK in PV using p38 gene silencing and targeted deletion of p38α MAPK in mouse epidermal keratinocytes.

Our studies indicate that p38α MAPK is not required for the loss of intercellular adhesion in PV. Mice with a targeted deletion of p38α MAPK in the epidermis develop suprabasal blisters after passive transfer of low and high doses of PV mAbs (Fig. 2 and supplemental Table S2), indicating that the loss of Dsg3-mediated adhesion is not p38α-dependent. Furthermore, Fig. 1 indicates that Dsg3 endocytosis does not require p38 activation and suggests that p38 MAPK activation is secondary to the loss of intercellular adhesion. Taken together, these findings suggest that PV mAbs directly inhibit Dsg3-mediated adhesion, a model that has previously been supported by *in vitro* assays (14).

It is possible but unlikely that other p38 isoforms could be mediating pathogenicity in our studies. Human keratinocytes express RNA for the α, β, and δ isoforms of p38 (32). Fig. 1 indicates that P2 and AK23 pathogenic antibodies do not activate any of these p38 isoforms. Mouse epidermal keratinocytes express p38α, p38γ, and p38δ isoforms (33). Fig. 2*C* indicates that only focal activation of p38δ was observed in

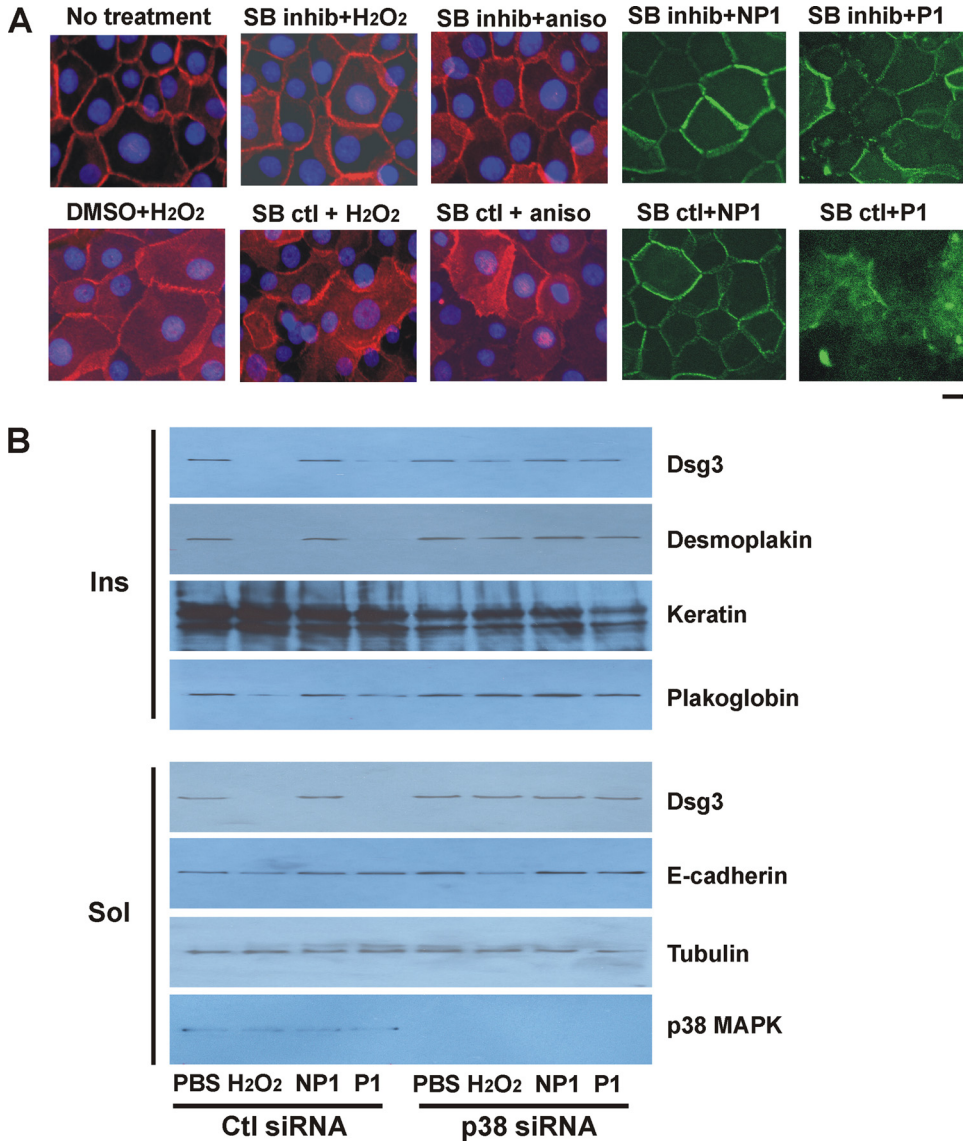

FIGURE 4. **Inhibition of p38 MAPK prevents Dsg3 endocytosis and depletion from desmosomal fractions.** *A*, p38 inhibition decreases internalization of Dsg3 by p38 activators and pathogenic PV mAbs. PHEK were pretreated with 2 μM SB202190 (p38 inhibitor (*inhib*)) or SB202474 (an inactive analog control) or the same volume of Me_2SO vehicle for 1 h, followed by 100 μg/ml anisomycin (*aniso*), 200 μM H_2O_2, or eGFP-conjugated nonpathogenic (NP1) or pathogenic (P1) PV mAb (200 μg/ml) for 4 h in medium containing 1.2 mM calcium. Subcellular localization of Dsg3 (*red*) or PV mAbs (*green*) was determined by immunofluorescence microscopy. p38 inhibition decreased the loss of cell surface Dsg3 caused by p38 activation and pathogenic PV mAbs. *Scale bar* = 10 μm. *B*, silencing of p38 MAPK expression prevents depletion of Dsg3 by oxidative stress or pathogenic PV mAb. PHEK were transiently transfected with siRNA specifically targeting p38 or a control (*Ctl*) siRNA for 48 h. Cells were treated with 200 μg/ml PV mAbs or 200 μM H_2O_2 for 4 h and lysed with buffer containing 1% Triton X-100. Protein levels in the Triton X-100-insoluble (*Ins*) and Triton X-100-soluble (*Sol*) fractions were determined by immunoblotting using specific antibodies as indicated. Data shown are representative of three independent experiments.

lesional keratinocytes of p38α-deficient mouse epidermis and that no activation was observed in perilesional keratinocytes, suggesting, similar to Fig. 1, that p38 activation is secondary to the loss of cell adhesion. Additionally, pyridinyl imidazole compounds such as SB202190 only inhibit p38α and p38β isoforms. However, definitive proof would require testing of mice with targeted deletion or inactivation of all p38 isoforms.

An unexpected finding in our study was that targeted deletion of p38α MAPK led to significant differences in the relative levels of cell surface Dsg3 observed in keratinocytes within the blister cavity (Fig. 2). For diagnostic studies on PV patients, direct immunofluorescence studies are performed on perilesional rather than lesional (*i.e.* blistered) epidermis because cell surface autoantibody staining is disrupted in keratinocytes within the blister cavity because of pathogenic autoantibody internalization. Similar to findings in PV patients, WT mice injected with pathogenic PV mAbs demonstrated loss of the linear cell surface IgG and Dsg3 staining pattern in lesional keratinocytes (Fig. 2*D*). In contrast, p38α-deficient keratinocytes within the blister cavity retained a significantly higher proportion of cell surface Dsg3 (Fig. 2*E*). These findings again support the model that the loss of intercellular adhesion does not depend on Dsg3 endocytosis. However, these data also indicate that Dsg3 endocytosis in the *in vivo* mouse model is impaired in the absence of p38α MAPK.

To further explore the relationship between p38 and Dsg3 endocytosis, we examined the effects of p38 activation, p38 inhibition, and p38 gene silencing in PHEK. If p38 activation

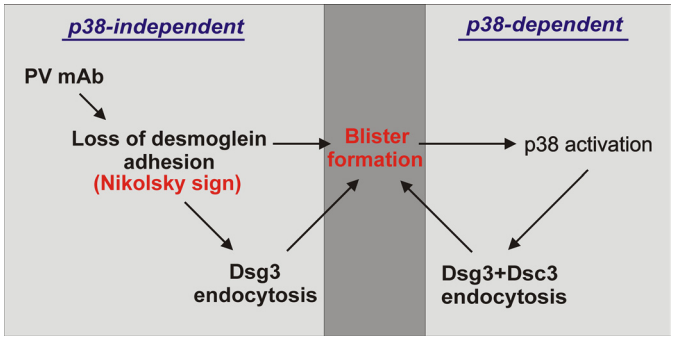

FIGURE 5. **Two-hit hypothesis for the role of p38 MAPK in PV pathogenesis.** Binding of PV mAbs to Dsg3 directly causes loss of desmoglein-mediated adhesion, leading to Nikolsky-positive blisters (Fig. 2). Pathogenic anti-Dsg3 PV mAbs cause Dsg3 (but not desmocollin 3) endocytosis (17), which is not always associated with p38 activation (Fig. 1). Loss of cell-cell adhesion subsequently activates p38, which promotes internalization of both Dsg3 and desmocollin 3 (Fig. 3) and depletion of multiple desmosomal molecules (Fig. 4). Therefore, PV mAbs cause the direct p38-independent loss of Dsg3-mediated adhesion, which is the initial pathogenic event in PV. These specific pathogenic effects are augmented by subsequent activation of p38 MAPK, leading to depletion of multiple desmosomal molecules, which may facilitate spontaneous blister formation in PV.

is upstream of Dsg3 endocytosis, then exogenous activation of p38 should cause Dsg3 endocytosis. p38 MAPK can be activated by the protein synthesis inhibitor anisomycin and also by oxidative stress induced by H_2O_2. Both anisomycin and oxidative stress caused internalization of cell surface Dsg3, Dsc3, and desmoplakin (Fig. 3), with no significant effect on the localization of the adherens junction protein E-cadherin at the same time points. The effects of anisomycin and H_2O_2 on Dsg3 internalization are likely due to p38 activation, as p38 inhibition by SB202190 blocked these effects (Fig. 4*A*).

Inhibition of p38α and p38β isoforms by SB202190 also at least in part blocked the pathogenic PV mAb-induced internalization of Dsg3. Similar findings using pyridinyl imidazole inhibitors and PV patient IgG have been described previously (23). To more specifically determine the dependence of H_2O_2- and PV mAb-induced loss of desmosomal Dsg3 on p38, we silenced total p38 expression in primary human keratinocytes. Knockdown of p38 expression rescued the PV mAb-induced depletion of desmosomal Dsg3 and, to a lesser extent, the oxidative stress-induced depletion of desmosomal Dsg3 (Fig. 4*B*).

Collectively, our studies support both p38-independent and p38-dependent mechanisms of pathogenicity in PV, leading to a "two-hit" model of disease (depicted in Fig. 5). PV mAbs directly cause the initial pathogenic event in PV: the loss of Dsg-mediated adhesion (Nikolsky's sign), which is p38-independent. Fig. 1*C* suggests that p38 activation is secondary to the loss of cell adhesion and also indicates a p38-independent mechanism of Dsg3 endocytosis. In contrast, Figs. 3 and 4 support a p38-dependent mechanism for Dsg3 endocytosis. A significant difference between these two mechanisms is that pathogenic PV mAbs cause endocytosis of Dsg3 but not Dsc3 (17), whereas exogenous activation of p38 leads to simultaneous loss of both cell surface Dsg3 and Dsc3. Pathogenic PV autoantibodies cause internalization of Dsg3 into an early endosomal compartment by a clathrin- and dynamin-independent mechanism (16–18). No significant colocalization of Dsg3 and early endosomal marker EEA-1 was observed in H_2O_2-treated keratinocytes, suggesting that these pathways may indeed differ. Future studies will aim to further elucidate the molecules and pathways regulating the turnover of cell surface Dsg3 under physiologic and pathophysiologic conditions.

The two-hit model is congruent with several observations on disease. First, it explains why p38 activation in a variety of skin diseases such as psoriasis does not lead to skin blistering (although loss of cell adhesion is observed in some skin cancers, such as acantholytic squamous cell carcinomas). It is also compatible with desmoglein compensation theory in that PV mAb-induced loss of desmoglein adhesion determines the site of pathology, with blister formation augmented by subsequent p38 activation. A prediction of the model is that p38 inhibition would ameliorate only p38-dependent pathologic processes (depicted on the *right* side of Fig. 5), which could be offset by increasing titers of pathogenic PV mAb (depicted on the *left* side of Fig. 5). In other words, clinical p38 inhibitors may work to prevent spontaneous blister formation but may not prevent skin fragility (Nikolsky positivity), particularly in severe cases with high titers of circulating pathogenic autoantibodies.

In summary, our data suggest that p38 activation and Dsg3 endocytosis are secondary to the loss of intercellular adhesion caused by pathogenic PV autoantibodies. Activation of p38 subsequently disrupts cell surface desmosomal cadherin localization, likely augmenting blister formation in PV. Targeting of p38 represents a novel treatment strategy for PV, which aims to block the target-organ pathologic response (*i.e.* increase keratinocyte adhesion) rather than generally suppress host immunity. Increased keratinocyte adhesion is thought to underlie the rapid therapeutic response of pemphigus patients to corticosteroids (42), although corticosteroids also cause immunosuppression and hyperglycemia, which are undesirable in patients with widespread blistering and risk of sepsis. Further study of pathways regulating keratinocyte adhesion may lead to safe and effective skin-targeted therapies for this life-threatening disorder.

Acknowledgments—We thank Andrea Stout, Elias Ayli, Tzvete Dentchev, John Seykora, and John Stanley for reagents, technical support, and scientific discussions.

REFERENCES

1. Payne, A. S., Hanakawa, Y., Amagai, M., and Stanley, J. R. (2004) *Curr. Opin. Cell Biol.* **16,** 536–543
2. Grando, S. A., Grando, A. A., Glukhenky, B. T., Doguzov, V., Nguyen, V. T., and Holubar, K. (2003) *J. Am. Acad. Dermatol* **48,** 86–92
3. Amagai, M., Klaus-Kovtun, V., and Stanley, J. R. (1991) *Cell* **67,** 869–877
4. Amagai, M., Karpati, S., Prussick, R., Klaus-Kovtun, V., and Stanley, J. R. (1992) *J. Clin. Invest.* **90,** 919–926
5. Amagai, M., Hashimoto, T., Shimizu, N., and Nishikawa, T. (1994) *J. Clin. Invest.* **94,** 59–67
6. Mahoney, M. G., Wang, Z., Rothenberger, K., Koch, P. J., Amagai, M., and Stanley, J. R. (1999) *J. Clin. Invest.* **103,** 461–468
7. Shirakata, Y., Amagai, M., Hanakawa, Y., Nishikawa, T., and Hashimoto, K. (1998) *J. Invest. Dermatol.* **110,** 76–78
8. Ding, X., Aoki, V., Mascaro, J. M., Jr., Lopez-Swiderski, A., Diaz, L. A., and Fairley, J. A. (1997) *J. Invest. Dermatol.* **109,** 592–596

9. Amagai, M., Tsunoda, K., Zillikens, D., Nagai, T., and Nishikawa, T. (1999) *J. Am. Acad. Dermatol.* **40,** 167–170
10. Miyagawa, S., Amagai, M., Iida, T., Yamamoto, Y., Nishikawa, T., and Shirai, T. (1999) *Br. J. Dermatol.* **141,** 1084–1087
11. Futei, Y., Amagai, M., Sekiguchi, M., Nishifuji, K., Fujii, Y., and Nishikawa, T. (2000) *J. Invest. Dermatol.* **115,** 829–834
12. Sekiguchi, M., Futei, Y., Fujii, Y., Iwasaki, T., Nishikawa, T., and Amagai, M. (2001) *J. Immunol.* **167,** 5439–5448
13. Al-Amoudi, A., Díez, D. C., Betts, M. J., and Frangakis, A. S. (2007) *Nature* **450,** 832–837
14. Heupel, W. M., Zillikens, D., Drenckhahn, D., and Waschke, J. (2008) *J. Immunol.* **181,** 1825–1834
15. Aoyama, Y., and Kitajima, Y. (1999) *J. Invest. Dermatol.* **112,** 67–71
16. Calkins, C. C., Setzer, S. V., Jennings, J. M., Summers, S., Tsunoda, K., Amagai, M., and Kowalczyk, A. P. (2006) *J. Biol. Chem.* **281,** 7623–7634
17. Mao, X., Choi, E. J., and Payne, A. S. (2009) *J. Invest. Dermatol.* **129,** 908–918
18. Delva, E., Jennings, J. M., Calkins, C. C., Kottke, M. D., Faundez, V., and Kowalczyk, A. P. (2008) *J. Biol. Chem.* **283,** 18303–18313
19. Sharma, P., Mao, X., and Payne, A. S. (2007) *J. Dermatol. Sci.* **48,** 1–14
20. Berkowitz, P., Hu, P., Liu, Z., Diaz, L. A., Enghild, J. J., Chua, M. P., and Rubenstein, D. S. (2005) *J. Biol. Chem.* **280,** 23778–23784
21. Berkowitz, P., Diaz, L. A., Hall, R. P., and Rubenstein, D. S. (2008) *J. Invest. Dermatol.* **128,** 738–740
22. Berkowitz, P., Hu, P., Warren, S., Liu, Z., Diaz, L. A., and Rubenstein, D. S. (2006) *Proc. Natl. Acad. Sci. U.S.A.* **103,** 12855–12860
23. Jolly, P. S., Berkowitz, P., Bektas, M., Lee, H. E., Chua, M., Diaz, L. A., and Rubenstein, D. S. (2010) *J. Biol. Chem.* **285,** 8936–8941
24. Han, J., Lee, J. D., Bibbs, L., and Ulevitch, R. J. (1994) *Science* **265,** 808–811
25. Lee, J. C., Laydon, J. T., McDonnell, P. C., Gallagher, T. F., Kumar, S., Green, D., McNulty, D., Blumenthal, M. J., Heys, J. R., and Landvatter, S. W. (1994) *Nature* **372,** 739–746
26. Freshney, N. W., Rawlinson, L., Guesdon, F., Jones, E., Cowley, S., Hsuan, J., and Saklatvala, J. (1994) *Cell* **78,** 1039–1049
27. Rouse, J., Cohen, P., Trigon, S., Morange, M., Alonso-Llamazares, A., Zamanillo, D., Hunt, T., and Nebreda, A. R. (1994) *Cell* **78,** 1027–1037
28. Jiang, Y., Chen, C., Li, Z., Guo, W., Gegner, J. A., Lin, S., and Han, J. (1996) *J. Biol. Chem.* **271,** 17920–17926
29. Mertens, S., Craxton, M., and Goedert, M. (1996) *FEBS Lett.* **383,** 273–276
30. Lechner, C., Zahalka, M. A., Giot, J. F., Møller, N. P., and Ullrich, A. (1996) *Proc. Natl. Acad. Sci. U.S.A.* **93,** 4355–4359
31. Jiang, Y., Gram, H., Zhao, M., New, L., Gu, J., Feng, L., Di Padova, F., Ulevitch, R. J., and Han, J. (1997) *J. Biol. Chem.* **272,** 30122–30128
32. Dashti, S. R., Efimova, T., and Eckert, R. L. (2001) *J. Biol. Chem.* **276,** 8059–8063
33. Kim, C., Sano, Y., Todorova, K., Carlson, B. A., Arpa, L., Celada, A., Lawrence, T., Otsu, K., Brissette, J. L., Arthur, J. S., and Park, J. M. (2008) *Nat. Immunol.* **9,** 1019–1027
34. Kumar, S., McDonnell, P. C., Gum, R. J., Hand, A. T., Lee, J. C., and Young, P. R. (1997) *Biochem. Biophys. Res. Commun.* **235,** 533–538
35. Goedert, M., Cuenda, A., Craxton, M., Jakes, R., and Cohen, P. (1997) *EMBO J.* **16,** 3563–3571
36. Fabian, M. A., Biggs, W. H., 3rd, Treiber, D. K., Atteridge, C. E., Azimioara, M. D., Benedetti, M. G., Carter, T. A., Ciceri, P., Edeen, P. T., Floyd, M., Ford, J. M., Galvin, M., Gerlach, J. L., Grotzfeld, R. M., Herrgard, S., Insko, D. E., Insko, M. A., Lai, A. G., Lélias, J. M., Mehta, S. A., Milanov, Z. V., Velasco, A. M., Wodicka, L. M., Patel, H. K., Zarrinkar, P. P., and Lockhart, D. J. (2005) *Nat. Biotechnol.* **23,** 329–336
37. Payne, A. S., Ishii, K., Kacir, S., Lin, C., Li, H., Hanakawa, Y., Tsunoda, K., Amagai, M., Stanley, J. R., and Siegel, D. L. (2005) *J. Clin. Invest.* **115,** 888–899
38. Amagai, M., Matsuyoshi, N., Wang, Z. H., Andl, C., and Stanley, J. R. (2000) *Nat. Med.* **6,** 1275–1277
39. Hanakawa, Y., Schechter, N. M., Lin, C., Garza, L., Li, H., Yamaguchi, T., Fudaba, Y., Nishifuji, K., Sugai, M., Amagai, M., and Stanley, J. R. (2002) *J. Clin. Invest.* **110,** 53–60
40. Ishii, K., Harada, R., Matsuo, I., Shirakata, Y., Hashimoto, K., and Amagai, M. (2005) *J. Invest. Dermatol.* **124,** 939–946
41. Tsunoda, K., Ota, T., Aoki, M., Yamada, T., Nagai, T., Nakagawa, T., Koyasu, S., Nishikawa, T., and Amagai, M. (2003) *J. Immunol.* **170,** 2170–2178
42. Nguyen, V. T., Arredondo, J., Chernyavsky, A. I., Kitajima, Y., Pittelkow, M., and Grando, S. A. (2004) *J. Biol. Chem.* **279,** 2135–2146